THE JOURNAL OF BIOLOGICAL CHEMISTRY
Vol. 276, No. 45, Issue of November 9, pp. 42389–42400, 2001

Printed in U.S.A.

The ORF3 Protein of Hepatitis E Virus Binds to Src Homology 3 Domains and Activates MAPK*

Received for publication, February 19, 2001, and in revised form, August 2, 2001
Published, JBC Papers in Press, August 22, 2001, DOI 10.1074/jbc.M101546200

Hasan Korkaya, Shahid Jameel‡, Dinesh Gupta, Shweta Tyagi, Ravinder Kumar, Mohammad Zafrullah, Manjari Mazumdar§, Sunil Kumar Lal, Li Xiaofang¶, Deepak Sehgal, Suman Ranjan Das, and Dinkar Sahal

From the International Centre for Genetic Engineering and Biotechnology (ICGEB), Aruna Asaf Ali Marg, New Delhi 110067, India and the §National Center for Biological Sciences, University of Agricultural Sciences-Gandhi Krishi Vigyan Kendra Campus, Bangalore 560065, India

The hepatitis E virus (HEV) is the causative agent of hepatitis E, an acute form of viral hepatitis. The biology and pathogenesis of HEV remain poorly understood. We have used *in vitro* binding assays to show that the HEV ORF3 protein (pORF3) binds to a number of cellular signal transduction pathway proteins. This includes the protein tyrosine kinases Src, Hck, and Fyn, the p85α regulatory subunit of phosphatidylinositol 3-kinase, phospholipase Cγ, and the adaptor protein Grb2. A yeast two-hybrid assay was used to further confirm the pORF3-Grb2 interaction. The binding involves a proline-rich region in pORF3 and the src homology 3 (SH3) domains in the cellular proteins. Competition assays and computer-assisted modeling was used to evaluate the binding surfaces and interaction energies of the pORF3·SH3 complex. In pORF3-expressing cells, pp60^{src} was found to associate with an 80-kDa protein, but no activation of the Src kinase was observed in these cells. However, there was increased activity and nuclear localization of ERK in the pORF3-expressing cells. These studies suggest that pORF3 is a viral regulatory protein involved in the modulation of cell signaling. The ORF3 protein of HEV appears to be the first example of a SH3 domain-binding protein encoded by a virus that causes an acute and primarily self-limited infection.

Hepatitis E virus (HEV),[1] the causative agent for hepatitis E, is a waterborne pathogen endemic to much of the developing world where it causes rampant sporadic infections and large scale epidemics (1–4). While the infection is self-limited with no associated chronicity, a fraction of the patients progress to fulminant hepatitis (5, 6), the most severe form of acute hepatitis. High mortality rates of 20–30% reported for HEV infection during pregnancy (7, 8) are also the result of fulminant hepatitis. The reasons for this and the mechanisms of viral pathogenesis are not known. The studies on HEV biology and pathogenesis have been severely restricted by the lack of a reliable cell culture system and small animal models of viral infection. We have used subgenomic expression strategies to study the properties and functions of individual HEV gene products toward understanding viral replication and pathogenicity (9–12).

The HEV genome is a ~7.5-kilobase polyadenylated, positive-sense RNA that contains three open reading frames (ORFs) designated ORF1, ORF2, and ORF3 (13). The ORF3 of HEV encodes a protein of ~13.5 kDa, called pORF3, for which no function has been assigned. When expressed in animal cells, pORF3 is phosphorylated at a single serine residue (Ser^{80}) in its 123-amino acid primary sequence (11). *In vitro* phosphorylation experiments suggested that pORF3 may be a substrate for the mitogen-activated protein (MAP) kinase, and subcellular fractionation revealed its association with the cytoskeleton (11). Recent results using inhibitors, activators, and dominant negative alleles show that pORF3 is a substrate for the extracellular signal-regulated kinase (ERK) as well as the stress-activated protein kinase/c-Jun N-terminal kinase members of the MAP kinase superfamily of enzymes.[2] These observations suggest a possible role for pORF3 in the cellular signal transduction pathway.

Another clue that pORF3 may have a potential role in cell signaling is the presence of proline-rich (P*XX*P) sequences, which are conserved among different isolates of HEV (Fig. 1). Such P*XX*P motifs are part of polyproline helices found in a number of viral and cellular proteins involved in signal transduction and bind the Src homology 3 (SH3) domains found in a diverse group of signal-transducing molecules (14, 15). Another well characterized modular signaling domain that mediates selective protein-protein interactions is the SH2 domain, which binds to phosphotyrosine-containing sequences (14, 15). The SH2/SH3 domain-containing enzymes and adaptors form distinct multiprotein complexes for transducing the extracellular signals to downstream effectors leading to the regulation of cellular responses (16, 17). A number of viral proteins are known to bind these host cell proteins to either interfere with or promote signal transduction for the benefit of viral replication, persistence, or evasion from host responses (18).

* This work was funded by internal support from the International Centre for Genetic Engineering and Biotechnology (ICGEB). The costs of publication of this article were defrayed in part by the payment of page charges. This article must therefore be hereby marked "*advertisement*" in accordance with 18 U.S.C. Section 1734 solely to indicate this fact.

‡ An International Senior Research Fellow in Biomedical Sciences of the Wellcome Trust. To whom correspondence should be addressed: Virology Group, ICGEB, Aruna Asaf Ali Marg, New Delhi 110067, India. Tel.: 91-11-6176680; Fax: 91-11-6162316; E-mail: shahid@icgeb.res.in.

¶ Present address: Hepatitis Branch, NCID/DVRD, Centers for Disease Control and Prevention, 1600 Clifton Rd., Atlanta, GA 30333.

[1] The abbreviations used are: HEV, hepatitis E virus; SH, Src homology; ERK, extracellular signal-regulated kinase; ORF, open reading frame; MAP, mitogen-activated protein; MAPK, MAP kinase; GST, glutathione *S*-transferase; PBS, phosphate-buffered saline; PMSF, phenylmethylsulfonyl fluoride; PAGE, polyacrylamide gel electrophoresis; BD, binding domain; AD, activation domain; SD, synthetic dextrose; MBP, myelin basic protein; PLC, phospholipase C; PI3K, phosphatidylinositol 3-kinase; TRE, tetracycline response element; HCV, hepatitis C virus; HIV, human immunodeficiency virus.

[2] S. Jameel, unpublished results.

Here we show that pORF3 binds some SH3 domain-containing proteins through one of its P*XX*P motifs. We have developed models for the binding of a proline-rich region in pORF3 to the SH3 domains of two proteins: c-Src, a protein tyrosine kinase, and Grb2, an adaptor protein. Further, in cells stably expressing pORF3, we present evidence for (*a*) specific association of an 80-kDa protein (p80) with pp60^{src} and (*b*) increased activity and nuclear localization of ERK, a member of the MAP kinase family of enzymes. The functional consequences of these observations for HEV pathogenesis are discussed.

EXPERIMENTAL PROCEDURES

Expression Vectors and Reagents—Vectors for the prokaryotic expression of glutathione *S*-transferase (GST)-fused SH3 domains were generously provided by Dr. I. Gout and Dr. M. J. Waterfield (Ludwig Institute for Cancer Research, London, United Kingdom), Dr. R. Ren (Brandeis University, Waltham, MA), and Dr. J. Chernoff (Fox Chase Cancer Center, Philadelphia, PA). The expression vector pRSET-ORF3 has been described previously (9). Plasmids pRSET-ORF3(Δ92–123), pRSET-ORF3(Δ78–123), and pRSET-ORF3(S80A) expressing mutant ORF3 proteins were generated by subcloning appropriate fragments (11) into plasmid pRSET-B (Invitrogen, Groningen, The Netherlands). Plasmid pRSET-ORF3(Mex), expressing an ORF3 protein from the Mexican isolate of HEV, contained a *Nco*I/*Eco*RI fragment from plasmid pBS-HEV-MRP14-1 (a kind gift of Dr. A. Tam, Genelab Technologies, Redwood City, CA) in pRSET-B. The vector for expression of ORF3 in animal cells, pMT-ORF3, has been described previously (12). For expression of pORF3 in insect cells, recombinant baculoviruses were constructed using the transfer vector pBacPak-ORF3.[3] The cloning of the *nef* gene of HIV-1 has been described elsewhere (19). Plasmid pRSET-Nef, expressing a full-length Nef protein from HIV-1 subtype C, was constructed by subcloning a ~650-base pair *Eco*RI/*Bam*HI *nef* fragment into plasmid pRSET-B. Polyclonal antibodies to the HEV ORF3 protein have been described previously (11). Other antibodies were obtained from the following sources: anti-v-Src (Ab-1) from Oncogene Research Products (Cambridge, MA) or anti-c-Src (SRC 2), anti-Src-agarose conjugate (N-16), and anti-Grb2 (C-7) from Santa Cruz Biotechnology (Santa Cruz, CA); anti-phosphotyrosine (PY99) and anti-ERK1 (K-23) from Santa Cruz Biotechnology; anti-p44/42 and anti-phospho-p44/42 from Cell Signaling Technology (Beverly, MA); and anti-hexahistidine tag from CLONTECH (Palo Alto, CA).

Cell Lines—The *ORF3* gene was subcloned as a *Bam*HI/*Hin*dIII fragment into the *Eco*RV site of the mammalian expression vector pcDNA1neo (Invitrogen). Following transfection of U2-OS human osteosarcoma cells with pcDNA-ORF3, colonies were selected with 800 μg/ml G418 (Life Technologies, Inc.). A number of independent clones were selected and screened for pORF3. Control cell lines stably integrated with the pcDNA1neo vector were similarly developed. The stable cell lines were propagated in Dulbecco's modified Eagle's medium containing 10% fetal bovine serum and 400 μg/ml G418. The COS-1, HEK293, and HepG2 cells were cultured in Dulbecco's modified Eagle's medium containing 10% fetal bovine serum and were transiently transfected as described elsewhere (10) and later under "Analysis of MAP Kinase Activity."

Preparation of Cell Lysates and Immunoprecipitation—Cells were grown in 60-mm dishes in Dulbecco's modified Eagle's medium containing 10% fetal bovine serum unless stated otherwise. Where required, serum starvation was carried out for 4–6 h in serum-free Dulbecco's modified Eagle's medium. Labeling of cells with [^{35}S]methionine/cysteine or [^{32}P]orthophosphate was carried out as described previously (11). For harvest, cells were washed with ice-cold PBS, and unless stated otherwise, the monolayers were dissolved in 1 ml of radioimmunoprecipitation buffer containing 1 mM PMSF and phosphatase inhibitors (1 mM Na_3VO_4 and 5 mM NaF). Wherever a protease inhibitor mixture was used, it included 16 μg/ml benzamidine, 10 μg/ml aprotinin, 10 μg/ml leupeptin, 10 μg/ml pepstatin A, 1 mM PMSF, and 10 μg/ml phenanthroline. The lysates were passed four times through a 23-gauge needle to shear the DNA and then centrifuged at 12,000 rpm and 4 °C for 10 min in a Biofuge 17RS (Heraeus, Hanau, Germany). For immunoprecipitation, the desired amount of supernatant was made up to 500 μl and immunoprecipitated with the primary antibodies for 1 h on ice followed by the addition of 100 μl of a washed 10% suspension of protein A-Sepharose and end-on mixing for 1 h at 4 °C. The immunoprecipitates were washed and analyzed further.

Protein Expression and Purification—The GST-SH3 fusion proteins were expressed in *Escherichia coli* DH5α and purified as described (20). The ORF3 protein was purified from *E. coli* as described previously (9). Sf21 insect cells were infected with ORF3 recombinant baculoviruses at an multiplicity of infection of 10, and the crude cell lysates were prepared in an extraction buffer containing 10 mM Tris-HCl, pH 7.5, 130 mM NaCl, 10 mM NaF, 10 mM $NaPP_i$, 1% Triton X-100, and the protease inhibitor mixture and were used for binding experiments. For purification of the Nef protein, pRSET-Nef/DH5α cells were washed with sonication buffer containing 50 mM sodium phosphate, pH 7.8, 300 mM NaCl, lysed by three freeze-thaw cycles in sonication buffer containing 10 μg/ml lysozyme and 1 mM PMSF, and sonicated four to five times with 1-min pulses. The clarified lysate was used to purify the Nef protein on nickel-nitrilotriacetic acid-agarose (Qiagen, Hilden, Germany) according to the recommendations of the supplier. The purified protein was eluted at 0.1–0.3 M imidazole.

In Vitro Binding Assays—For the GST pull-down assay, glutathione-Sepharose beads (Amersham Pharmacia Biotech) containing 2 μg of bound GST-SH3 were mixed with either 2 μg of *E. coli*-expressed pORF3 or a lysate from 1×10^6 Sf21 insect cells in 500 μl of a GST binding buffer containing 20 mM Tris-HCl, pH 7.9, 180 mM KCl, 5 mM $MgCl_2$, 0.2 mM EDTA, 1 mM dithiothreitol, 1 mM PMSF, 0.1% Nonidet P-40, and 1 mg/ml bovine serum albumin. After incubation with mixing at 4 °C for 90 min, the beads were washed six times with GST binding buffer containing 0.2% Nonidet P-40 but no bovine serum albumin. The bound proteins were subjected to SDS-PAGE and Western blotting with anti-ORF3 antibodies. For the filter binding assay, 2 μg of each GST-SH3 fusion protein were subjected to SDS-PAGE, and the proteins were transferred to a nitrocellulose membrane. The membrane was incubated overnight at 4 °C in GST binding buffer with about 30 μg of purified, biotinylated ORF3 protein. Biotinylation of pORF3 and subsequent Western blotting and detection steps were carried out with an ECL Protein Biotinylation Module (Amersham Pharmacia Biotech) according to the recommendations of the supplier.

Competition of Binding—Glutathione-Sepharose beads containing 2 μg of the GST-SH3(Hck) fusion protein were mixed with 5 μg of purified pORF3 in the presence of increasing amounts of a 30-mer peptide (amino acids 92–121 of the Indian ORF3 sequence, Fig. 1*B*). Alternatively, increasing amounts of the peptide were preincubated with the fusion protein-carrying beads at 4 °C for 30 min prior to the addition of pORF3. For competition between pORF3 and Nef for SH3 domain binding, 3 μg of pORF3 and increasing amounts of Nef were co-incubated with beads containing 2 μg of the fusion protein. Alternatively, 3 μg of Nef and increasing amounts of pORF3 were used. The binding and washes were carried out as described above for the GST pull-down assay. The beads were boiled in loading dye and analyzed by SDS-PAGE followed by either Coomassie Blue staining or Western blotting. Densitometric analysis was carried out with the Kodak ID Image Analysis Software (Kodak Digital Science).

Yeast Two-hybrid Assay—The *ORF3* and *Grb2* genes were cloned in-frame in the GAL4 DNA binding domain (BD) and activation domain (AD) vectors, respectively. For *ORF3*, a *Sma*I/*Bam*HI fragment from plasmid pSG-ORF3 (10) was cloned into plasmid pGBT9 (21) to give pBD-ORF3. The truncated ORF3 mutant (Δ80–123) was constructed by digesting pBD-ORF3 with *Eag*I and *Bam*HI and religation of the remaining vector. For *Grb2*, a *Bam*HI/*Not*I fragment from plasmid pGEX-Z1-Grb2 was first cloned into plasmid pSGI (10); a *Pst*I fragment was then cloned into plasmid pGAD424 (21) to give pAD-Grb2. *Saccharomyces cerevisiae* strain Y190 (*MAT**a*** *trp1-901 his3 leu2-3,112 ura3–52 ade2 gal4 gal80 URA3*::*GAL-lacZ LYS2*::*GAL-HIS3*) cells were co-transformed by the LiCl method (22) with pAD-Grb2 and pBD-ORF3. Y190 contains integrated copies of both *HIS3* and *lac*Z reporter genes under the control of GAL4 binding sites. Single and co-transformants were plated on synthetic dextrose medium lacking tryptophan, leucine, and histidine (SDTrp$^-$Leu$^-$His$^-$) to select for clones in which the *HIS3* gene was transactivated. Appropriate positive and negative controls were used. The β-galactosidase assays were carried out as described previously (22).

Immunofluorescence Analysis—The cells were plated at a confluency of about 50% on coverslips in six-well plates and grown for 18 h. The PBS-washed cells were fixed with 2% paraformaldehyde in PBS at room temperature for 10 min, permeabilized with 100% methanol at −20 °C for 3 min, and then rehydrated with PBS for 20 min at room temperature. The cells were blocked with 5% normal donkey or goat serum for 2 h at room temperature and then incubated with appropriately diluted primary antibodies in PBS/0.5% Tween 20 (PBST) containing 1% normal serum for 2 h at room temperature. The primary antibodies used were monoclonal or polyclonal anti-ORF3 at 1:200 to 1:500, polyclonal

[3] D. Sehgal, unpublished results.

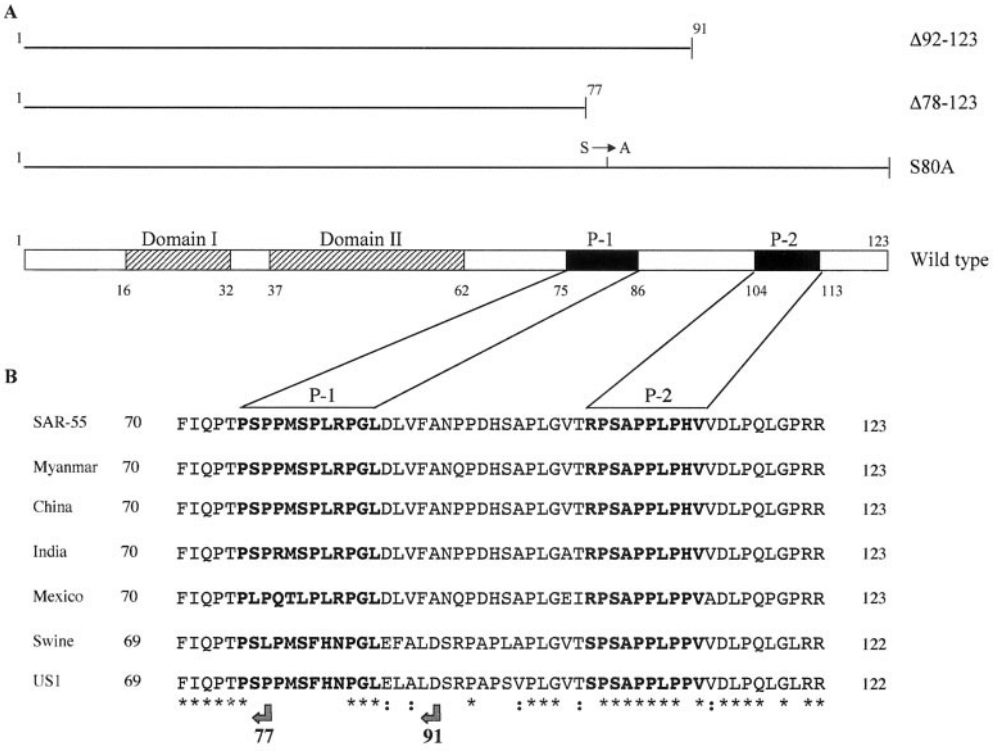

FIG. 1. **The ORF3 protein and conserved domains.** *A*, the ORF3 protein and its mutants are illustrated with two N-terminal hydrophobic domains (*Domain I* and *II*) and two C-terminal proline-rich regions (*P-1* and *P-2*). The *numbers* indicate the amino acids at the boundaries of the various domains, regions, and mutants. The mutant S80A carries a Ser to Ala mutation at amino acid 80. *B*, the C-terminal amino acid sequences of the ORF3 proteins from various geographically distinct isolates of HEV are shown. The sequences of P-1 and P-2 regions are marked and shown in *bold type*. The amino acid residues conserved across all isolates (*) and conservative changes (:) are marked.

anti-c-Src at 1:500 or 1:1000, or monoclonal anti-Grb2 at 1:400. Cells were washed thrice with PBST for 5 min each and then incubated for 1 h at room temperature with a 1:1000 dilution of conjugated secondary antibodies. For colocalization experiments, the secondary antibodies used were goat anti-rabbit IgG or goat anti-mouse IgG coupled to either Alexa488 or Alexa594 dyes (Molecular Probes, Eugene, OR). These were chosen to always label pORF3 with Alexa488 (green) and Src or Grb2 with Alexa594 (red). For the MAPK and phospho-MAPK localization experiments, the secondary antibodies used were Cy3-conjugated donkey anti-rabbit or anti-mouse (Jackson Laboratories, Bar Harbor, ME) or fluorescein isothiocyanate-conjugated goat anti-rabbit (DAKO, Glostrup, Denmark). Cells were washed as described earlier and mounted in 90% glycerol in PBS. Confocal images were collected using a 60× or 100× planapo objective in a Bio-Rad 1024 LSM attached to a Nikon inverted microscope. To prevent cross-talk in dual labeling experiments, only one dye was excited at a time, keeping the other channel completely closed. The images were processed in Confocal Assistant followed by Adobe Photoshop version 5.0.

Molecular Modeling—The three-dimensional structures of known SH3·ligand complexes from the Protein Data Bank (PDB) were used for generating a scaffold. For modeling the HEV pORF3 peptide RPSAPPLPHV (P-2) bound to the Src SH3 domain, the structure of c-Src complexed with the class I peptide RALPPLPRY (called RLP2) was used as a guiding model (PDB code 1RLQ). The complexes were energy minimized using AMBER (version 6.0) along with the forcefield parameters of Cornell *et al.* (23). This included 500 steps of steepest descent minimization followed by 500 steps of conjugate gradient minimization. A 10-Å cut-off for the nonbonded interactions and a distance-dependent dielectric constant were used. Subsequently the energy-minimized complex was solvated with a 5-Å shell of TIP3P water molecules. Torsion angle and interaction energy analysis was done using ANAL (AMBER version 6.0). The final models were displayed using INSIGHT-II (Molecular Simulations Inc.). A similar strategy was used to model the complex of P-2 and the Grb2 SH3 domain (PDB code 1SEM).

Analysis of pp60^{src} Activity—The immune complex Src kinase assays were carried out as follows. Control pCneo and pORF3-expressing cells were lysed in a buffer containing 20 mM Tris-HCl, pH 8.0, 150 mM NaCl, 2.5 mM EDTA, 1% Nonidet P-40, 1 mM PMSF, 10 μg/ml aprotinin, 10 μg/ml leupeptin, 1 mM Na_3VO_4, and 5 mM NaF. The cell lysates were quantitated for protein content using the Bradford Reagent (Bio-Rad), and an equivalent amount of each lysate was immunoprecipitated with 1 μg of agarose-conjugated anti-Src antibodies for 2 h at 4 °C with end-on mixing. The beads were washed twice with lysis buffer and once with kinase buffer containing 20 mM HEPES, pH 7.4, 10 mM $MnCl_2$, and phosphatase inhibitors. The washed beads were then resuspended in 30 μl of kinase buffer containing 10 μg of acid-denatured enolase and 10 μCi of [γ-^{32}P]ATP and incubated at 30 °C for 30 min. The reaction was terminated with 10 μl of 6× SDS dye, boiled for 4 min, and subjected to SDS-12% polyacrylamide gel electrophoresis. The proteins were transferred to a nitrocellulose membrane, which was then exposed to an x-ray film.

Analysis of MAP Kinase Activity—The MAP kinase activity in cell lysates was assayed with a p44/42 MAP Kinase Assay kit (Cell Signaling Technology) according to the recommendations of the supplier. This assay measured phosphorylation of the ERK substrate Elk-1. Alternatively an immunoprecipitation kinase assay was also carried out using myelin basic protein (MBP) as a substrate. Equivalent amounts of each lysate were immunoprecipitated with 1 μg of the anti-ERK1 antibody and protein A-Sepharose as described above. The beads were washed thrice with radioimmunoprecipitation buffer containing protease and phosphatase inhibitors and once with a kinase buffer containing 50 mM Tris-HCl, pH 7.4, 150 mM NaCl, 10 mM $MgCl_2$, 1 mM dithiothreitol, 100 μg/ml bovine serum albumin, 1 mM PMSF, and 20 mM NaF. The beads were then resuspended in 25 μl of kinase buffer containing 10 μg of MBP and 10 μCi of [γ-^{32}P]ATP and incubated at 30 °C for 30 min. The reaction was terminated with 25 μl of 2× SDS dye, heated at 95 °C for 5 min, and subjected to SDS-15% polyacrylamide gel electrophoresis. The proteins were transferred to a nitrocellulose membrane, which was then exposed to an x-ray film.

The MAPK activity in transfected cells was determined using the *In Vivo* MAP Kinase Assay System (CLONTECH) according to the guidelines of the supplier. HEK293 cells were seeded at about 50% confluency in wells of a six-well plate the day before transfection. The cells were co-transfected with the required expression vectors using Lipofectin (Life Technologies, Inc.) as described previously (10). In a typical experiment to study the effect of pORF3 expression on cellular MAPK activity, cells in each well were co-transfected with three vectors: the transactivator vector pTet-Elk-1 (50 ng), the reporter vector pTRE-Luc (1 μg), and the ORF3 expression vector pMT-ORF3 (50 ng). All transfections were carried out in duplicates or triplicates. Other controls

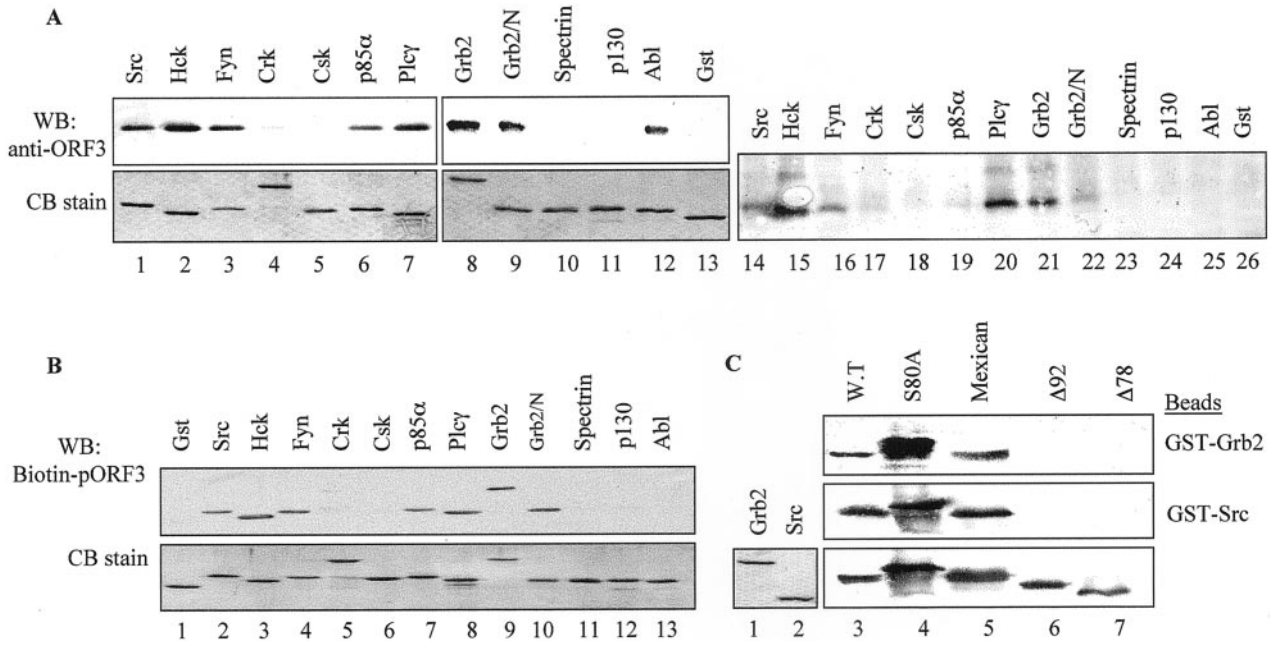

FIG. 2. ***In vitro* binding of pORF3 to SH3 domains.** *A*, GST pull-down assay. Purified GST-SH3 fusion proteins were used to trap pORF3 expressed in either *E. coli* (*lanes 1–13*) or insect cells (*lanes 14–26*) as described under "Experimental Procedures." For *lanes 1–13*, the *upper panel* shows a Western blot with anti-pORF3 antibodies; the *lower panel* shows a Coomassie Blue-stained gel for GST-SH3 proteins. *Lanes 14–26* show a Western blot for pORF3 detection; the GST-SH3 proteins used were the same shown in *lanes 1–13*, *lower panel*. *B*, filter binding assay. The GST-SH3 fusion proteins were subjected to SDS-PAGE followed by either Western blotting with a biotinylated ORF3 protein (*upper panel*) or Coomassie Blue staining (*lower panel*). *C*, mapping of the SH3-binding region in pORF3. The wild type or mutant ORF3 proteins (*bottom panel*) were used in a pull-down assay either with GST-SH3(Grb2) (*upper panel*) or GST-SH3(Src) (*middle panel*). The bound proteins were resolved by SDS-PAGE and Western blotted with anti-hexahistidine tag antibodies. *Lanes 1* and *2* show a Coomassie Blue-stained gel for GST-SH3(Grb2) and GST-SH3(Src). *WB*, Western blot; *CB*, Coomassie Blue; *W.T*, wild type.

included transfections with 50 ng of plasmid pTet-Neg or pMT3 (expression vector for ORF3) to determine background signals or plasmid pTet-Off as positive control. Six hours post-transfection, cells were switched to complete medium containing 10% fetal bovine serum and grown for an additional 12 h. The cells were then serum-starved for 24 h during which time some control cells were incubated with 2 μg/ml doxycycline for 12 h to ensure that the response was mediated by the Tet transactivator. Cell were washed twice with PBS without Ca^{2+} and Mg^{2+}, and lysates were prepared in 200 μl of Cell Lysis Buffer supplied with the Luciferase Reporter Assay kit (CLONTECH) according to the instructions of the supplier. Twenty microliters of each lysate was then assayed for luciferase activity as instructed in the assay manual.

RESULTS

pORF3 Binds SH3 Domains in Vitro—Two C-terminal proline-rich regions, P-1 (amino acids 75–86) and P-2 (amino acids 104–113), are conserved in pORF3 from various isolates of HEV (Fig. 1). Because similar P*XX*P motifs, including those found in other viral proteins, bind to SH3 domains found in signaling proteins, we tested the ability of pORF3 to interact with these domains from a number of such proteins. In a GST pull-down assay, pORF3 expressed in *E. coli* or insect cells bound to SH3 domains from Src family tyrosine kinases Src, Hck, and Fyn and the signaling proteins Grb2 and phospholipase Cγ (PLCγ) (Fig. 2*A*). No binding was observed with GST alone or with SH3 domains from Csk, Spectrin, and p130^{cas}, while weak binding was observed with the SH3 domains of the p85α regulatory subunit of phosphatidylinositol 3-kinase (PI3K) and Crk although equivalent amounts of GST-SH3 fusion proteins were used to trap pORF3 on beads (Fig. 2*A*, *lower panel*). The interactions were also evaluated independently by a filter binding assay (Fig. 2*B*), the results being consistent with those from the GST pull-down assay. The only exception was the SH3 domain of Abl, which bound to *E. coli*-expressed but not to insect cell-expressed pORF3 in the GST pull-down assay (Fig. 2*A*, *lanes 12* and *25*); no binding was observed in the filter binding assay as well (Fig. 2*B*, *lane 13*). The binding of pORF3 to other SH3 domains was both specific and reproducible between the two assays.

To test which of the two P*XX*P regions in pORF3 bound SH3 domains, we carried out GST pull-down assays using mutant ORF3 proteins (Fig. 1) and fusion proteins containing the Grb2 or Src SH3 domains. While the wild type pORF3 bound Grb2 and Src SH3 domains (Fig. 2*C*, *lane 3*), the Δ92–123 or the Δ78–123 mutants did not (Fig. 2*C*, *lanes 6* and *7*). A mutant of pORF3 in which Ser^{80} (in the P-1 region) was changed to alanine as well as pORF3 from the Mexican isolate of HEV, containing a conserved P-2 region but a variant P-1 region, also bound the GST-SH3(Grb2) and GST-SH3(Src) fusion proteins (Fig. 2*C*, *lanes 4* and *5*, respectively). The Δ92–123 protein did not bind to any of the GST-SH3 fusion proteins in our panel in either of the two assays used (data not shown). These results showed the P-2 region of pORF3 to be necessary for its binding to SH3 domains.

Competition Analysis of pORF3 Binding to SH3 Domains—The binding of pORF3 to SH3 domains was further characterized by competition with a 30-mer synthetic peptide. Although the peptide included the entire P-2 region and its flanking sequences, it competed very poorly with the full-length ORF3 protein for SH3 domain binding (Fig. 3*A*). Only at a 1000-fold molar excess of the peptide was there up to 90% reduction in pORF3 binding when the peptide was preincubated with the GST-SH3(Hck) beads prior to pORF3 binding. However, when pORF3 and the peptide were co-incubated with GST-SH3(Hck) beads, protein binding was reduced only by about 50% at a 1000-fold molar excess of the peptide. Thus, compared with pORF3 a peptide encompassing the P-2 region bound SH3 domains with reduced affinity.

The interaction of HIV-1 Nef with SH3 domain-containing cellular proteins has been characterized in detail, and the binding affinities have been measured. Since Nef binds the Hck SH3 domain with high affinity, we carried out a competition

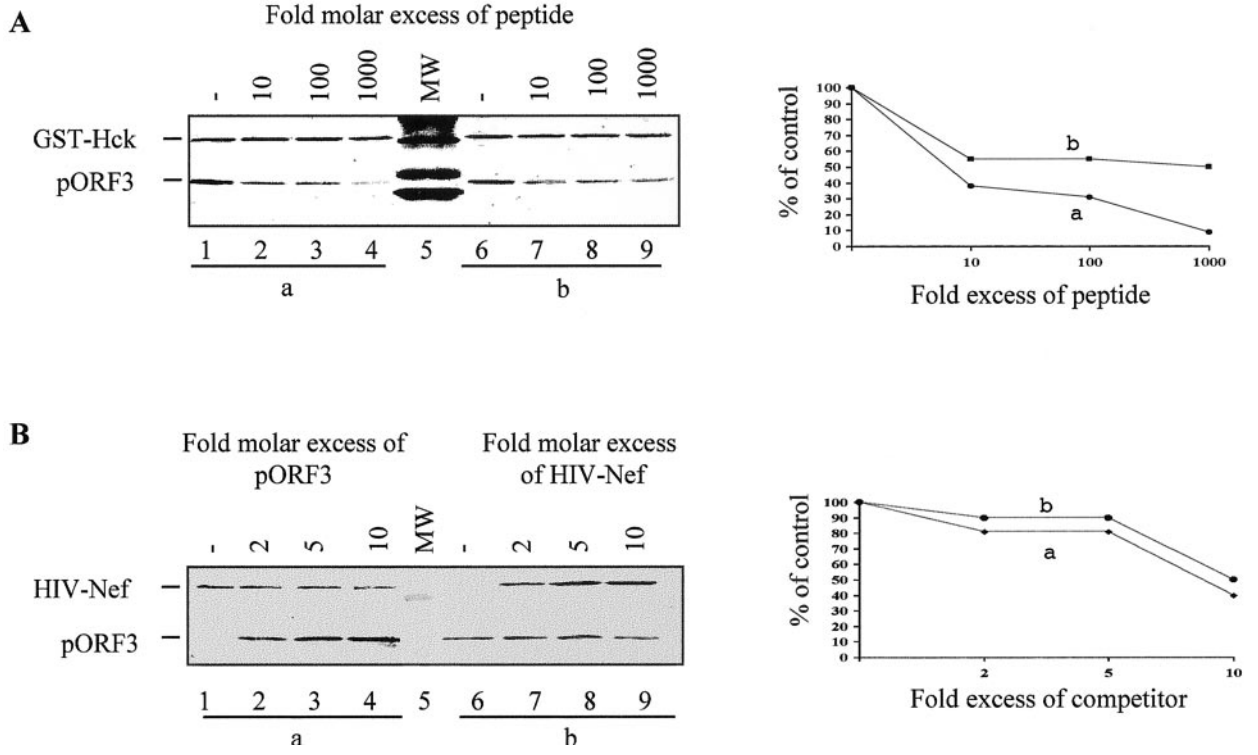

FIG. 3. **Competition analysis of pORF3 binding to GST-SH3(Hck).** *A*, competition with peptide. Glutathione-Sepharose beads containing 2 μg of GST-SH3(Hck) were incubated with 5 μg of pORF3 and an increasing molar excess of a 30-mer peptide encompassing amino acids 92–121 of pORF3. The peptide was either preincubated with GST-SH3(Hck) prior to pORF3 addition (*a*, *lanes 1–4*), or the peptide and pORF3 were co-incubated with GST-SH3(Hck) (*b*, *lanes 6–9*). The pORF3 retained on beads was estimated by SDS-PAGE and Coomassie Blue staining. The molecular size markers (*MW*, *lane 5*) shown are 14.3, 21.5, and 30 kDa from *bottom to top*. The position of GST-SH3(HcK) and pORF3 are indicated. *B*, competition with Nef. Beads carrying GST-SH3(Hck) were incubated either with 3 μg of Nef and increasing amounts of pORF3 (*a*, *lanes 1–4*) or with 3 μg of pORF3 and increasing amounts of Nef (*b*, *lanes 6–9*). The proteins retained on beads were Western blotted with anti-hexahistidine tag antibodies. The molecular size marker (*MW*, *lane 5*) corresponding to 29 kDa is seen. The positions of Nef and pORF3 are indicated. In both competition experiments, the bands were quantitated by densitometry, and the results are shown on the *right*.

analysis for binding of pORF3 and Nef to the GST-SH3(Hck) target. The results showed that pORF3 and Nef were equally effective in competing with each other for binding to the Hck SH3 domain (Fig. 3*B*).

Yeast Two-hybrid Analysis—To test if the interaction of pORF3 with SH3 domains took place *in vivo* as well, we used the yeast two-hybrid system and chose Grb2 as an example of the interacting partner. The AD-Grb2 and BD-ORF3 constructs were expressed singly or together in cells carrying the *HIS3* and β-galactosidase (*lacZ*) reporter genes. An interaction between hybrid proteins was scored by the capacity of yeast cells to grow on medium lacking histidine (His^-). The results are presented in Fig. 4. All cells grew on YPD (yeast extract, 10 g/liter; peptone, 20 g/liter; dextrose, 20 g/liter) medium showing that the transformed yeast cells were viable and the expressed fusion proteins did not inhibit growth (Fig. 4*B*). Cells transformed with single vectors either carrying the GAL4 DNA binding domain (with *trp1* auxotrophic marker) or the GAL4 activation domain (with *leu3* auxotrophic marker) were able to grow on synthetic medium lacking tryptophan ($SDTrp^-$) or leucine ($SDLeu^-$), respectively (Fig. 4, *C* and *D*). Only cells co-transformed with AD-Grb2/BD-ORF3 vectors or the positive control vectors (SNF1/SNF4) grew on synthetic medium lacking leucine, tryptophan, and histidine ($SDLeu^-Trp^-His^-$) (Fig. 4*E*). Over 100 His^+ colonies were obtained on co-transformation with AD-Grb2 and BD-ORF3 vectors. Most of these cells also showed β-galactosidase activity. The results of only two representative colonies are shown (Fig. 4*F*). The binding of BD-ORF3 and AD-Grb2 fusion proteins was specific since (*a*) the former did not bind the GAL4 AD alone and the latter did not bind the GAL4 BD alone (results not shown), (*b*) the GAL4 activation and binding domains by themselves do not interact with each other, and (*c*) the BD-ORF3 fusion proteins expressed from two independent clones of plasmid pGBT9-ORF3 bound to the AD-Grb2 fusion protein. A truncated pORF3, lacking amino acid residues 80–123 and both the P-1 and P-2 regions, also did not show any interaction with full-length Grb2. These results confirmed that *in vivo* pORF3 also bound a SH3 domain-containing protein, Grb2, and that this binding was dependent upon proline-rich regions in the C-terminal part of pORF3.

Colocalization of pORF3 and Cellular Proteins—In dual labeling experiments we studied the colocalization of pORF3 and either Src or Grb2 in (*a*) COS-1 cells transiently transfected with the expression vector pMT-ORF3 or (*b*) cell lines stably expressing pORF3. The distribution of pORF3 in these cells was cytoplasmic and displayed punctate staining (Fig. 5). When an enhanced green fluorescent protein-fused form of pORF3 was expressed transiently in Huh7 liver cells, a similar localization pattern was observed in live cells.[2] This ensured that pORF3 staining was not an artifact of fixing the cells or its overexpression in stable cell lines and that its distribution in nonhepatic cells was similar to that in hepatic cells. The Src protein was found all over the cell in the cytoplasmic as well as the nuclear compartments, while the Grb2 protein was primarily localized to the cytoplasmic regions (Fig. 5). Distinct orange or yellow staining regions were observed in the merged images indicative of the colocalization of pORF3 with either Src or Grb2 (Fig. 5, *arrows*). This was further confirmed by carrying out line scans of the images during confocal microscopy separately in the green and red channels.

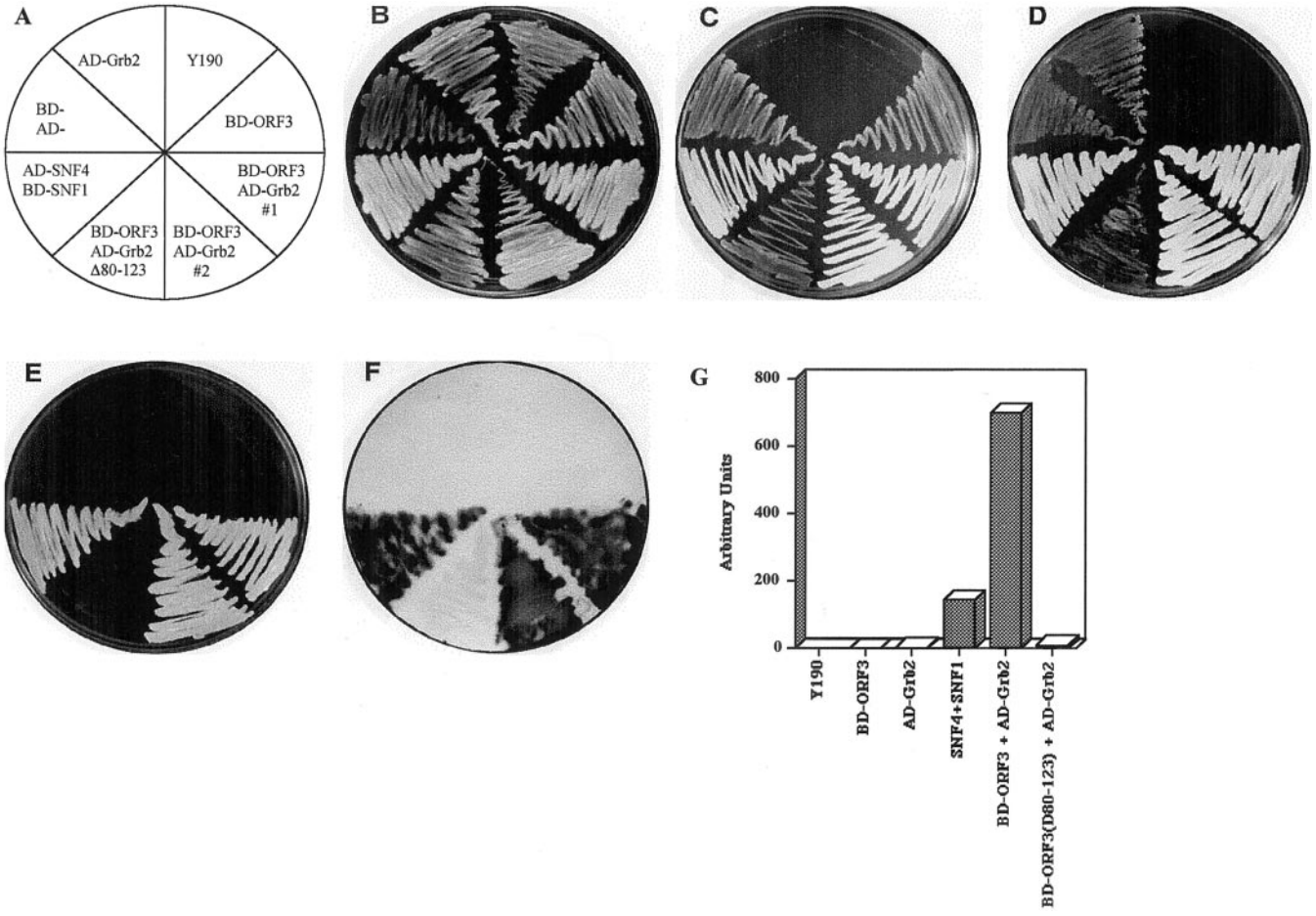

FIG. 4. **Yeast two-hybrid analysis of pORF3 binding to Grb2.** The yeast two-hybrid analysis was carried out as described under "Experimental Procedures." Panels show the plating pattern (*A*) and growth on YPD (*B*) or on synthetic medium lacking tryptophan (*C*), leucine (*D*), or leucine, tryptophan, and histidine (*E*). β-galactosidase expression in cells grown on YPD is shown on a filter (*F*) or in a liquid assay (*G*).

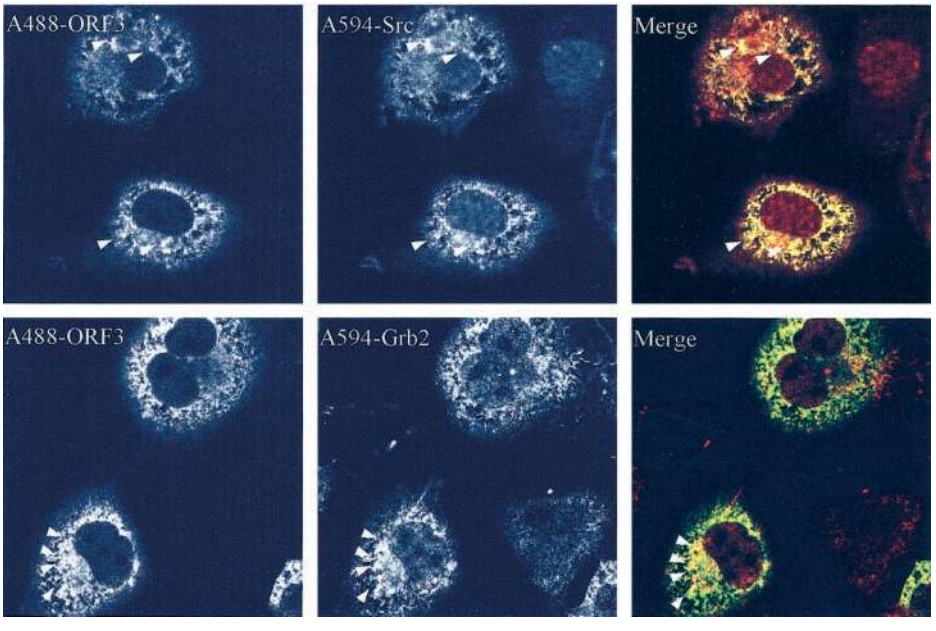

FIG. 5. **Colocalization of pORF3 and SH3 domain proteins.** COS-1 cells transiently transfected with pMT-ORF3 were doubly labeled with monoclonal anti-pORF3 and polyclonal anti-c-Src (*top panels*) or with polyclonal anti-pORF3 and monoclonal anti-Grb2 (*bottom panels*) followed by the Alexa488 (*A488*)- or Alexa594 (*A594*)-conjugated anti-rabbit IgG or anti-mouse IgG antibodies. Separate images were acquired as described under "Experimental Procedures" and were then merged using the Adobe Photoshop version 5.0 software. *Arrows* indicate regions of overlap.

Molecular Modeling of pORF3 Binding to SH3 Domains—The P-2 peptide was modeled on the three-dimensional structures of the c-Src and Grb2 SH3 domains (24, 25). The energy-minimized solvated structures are shown in Fig. 6. For comparison, the binding surfaces of P-2 with Src and Grb-2 SH3 domains are shown along with those for the PDB 1RLQ and 1SEM structures. The interaction energies for Src SH3 domain binding to P-2 and the RLP2 ligands were calculated to be −76.5 and −70.3 kcal/mol, respectively; the Grb2 SH3 domain bound the P-2 and mSOS ligands with interaction energies of −73.8 and −85.8 kcal/mol, respectively. The P-2 peptide binds to the hydrophobic recognition platform in the SH3 do-

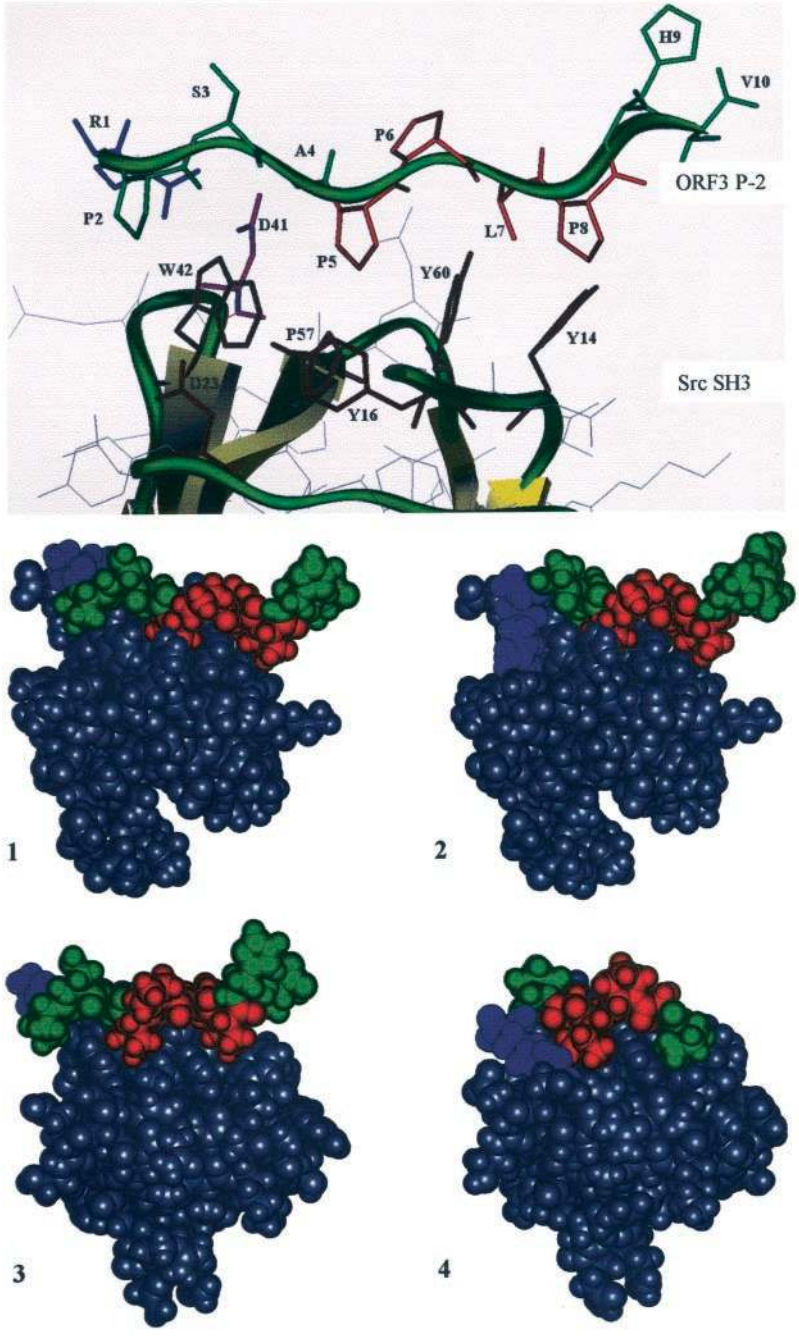

FIG. 6. **Model of c-Src SH3 domain binding to the ORF3 P-2 peptide.** The energy-minimized solvated models are shown for the Src SH3 with P-2 (*1*) or RLP2 (*2*) and for the Grb2 SH3 with P-2 (*3*) or mSOS (*4*). The SH3 domains are shown in *gray*. In the peptide ligand, the hydrophobic core is *orange*, the salt-bridging Arg is *blue*, and the noninteracting residues are *green*. The *upper panel* shows side chains in P-2 interacting with Src SH3 binding pockets.

main with the same conformation in both Src and Grb2. In both models, residues 2–8 of P-2 form a polyproline II helix, with three residues per turn. Analogous to other polyproline II helices, the P-2 peptide shows an (i, i+3) arrangement of prolines with the flanking prolines in the PPLP sequence on the same face of the helix. Pro^{2}, Pro^{5}, and Pro^{8} in P-2 form one face of the helix that interacts with the SH3 domain, Ala^{4} and Leu^{7} are on the other face, while Ser^{3}, Pro^{6}, and His^{9} project away from the helix (Fig. 6, *upper panel*). The ligand binding site on the c-Src SH3 domain has been shown to contain three binding pockets. The first one, formed by Tyr^{14} and Tyr^{60}, interacts with Leu^{7} and Pro^{8} of the P-2 peptide. Residues Tyr^{16}, Trp^{42}, Pro^{57}, and Tyr^{60} form the second pocket that makes hydrophobic interactions with Ala^{4} and Pro^{5} of P-2. The third pocket binds the Arg^{1} residue in a salt bridge with a conserved aspartate. While in the PDB 1RLQ structure this interaction is with Asp^{23}, the P-2 peptide interacts with the conserved Asp^{41} in the c-Src SH3 domain. Residues C-terminal to the proline-rich core, His^{9} and Val^{10} in P-2 or Arg^{8} and Tyr^{9} in the RLP2 ligand, do not bind the c-Src SH3 domain. Similar sets of contacts were found in the model for P-2 binding to the Grb2 SH3 domain. In the PDB 1SEM structure Arg^{1} of the peptide interacts with $Glu1^{72}$, while the Arg^{1} of peptide P-2 interacts with the conserved Asp^{188} of the Grb2 SH3 domain.

Modeling of the P-2 peptide with c-Src and Grb2 SH3 domains and a comparison of these models with the PDB 1RLQ and 1SEM structures showed that the P-2 region bound similarly in the two structures (Fig. 6). The proline-rich core of P-2 was buried in each of the SH3 domains, and this binding caused minimal structural deformity of the SH3 domains. The arginine (Arg^{1}) present at the N terminus of the P*XX*P motif formed salt bridges in both structures, although with conserved residues other than those found in the PDB structures.

pORF3 Binds but Does Not Activate the Src Kinase—The binding of proteins containing a P*XX*P motif to the SH3 domain

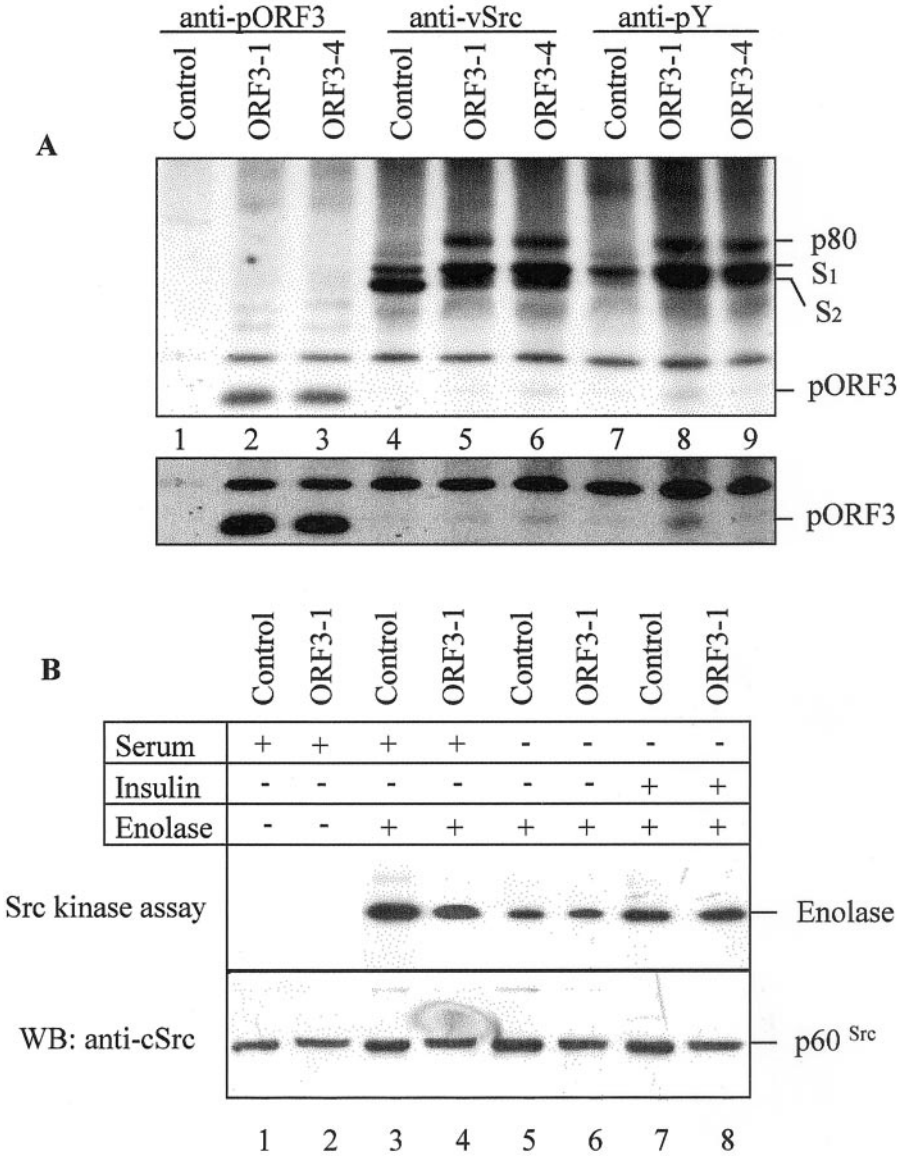

FIG. 7. **Effect of pORF3 on c-Src.** *A*, control or pORF3-expressing (*ORF3-1* and *ORF3-4*) stable cell lines were labeled with [^{32}P]orthophosphate. The cells lysates were immunoprecipitated with anti-ORF3 (*lanes 1–3*), anti-v-Src (*lanes 4–6*), or anti-phosphotyrosine (*anti-pY*) (*lanes 7–9*) antibodies. S1 and S2 indicate two differentially phosphorylated forms of pp60^{src}; p80 indicates a coprecipitating cellular protein. The position of pORF3 is indicated. The *lower panel* shows a longer exposure of the *bottom* part of the gel. *B*, lysates were prepared from control (*lanes 1*, *3*, *5*, and *7*) and pORF3-expressing (*lanes 2*, *4*, *6*, and *8*) cells that were either cultured in complete medium containing 10% fetal bovine serum (*lanes 1–4*) or were serum-starved for 12 h (*lanes 5–8*). One set of serum-starved cells were induced with 1 μM insulin for 1 h (*lanes 7* and *8*). The cell lysates were subjected to an immunoprecipitation kinase assay for Src kinase using acid-denatured enolase as a substrate as described under "Experimental Procedures." No enolase was added to reactions shown in *lanes 1* and *2*. The same cell lysates were Western blotted with an antibody to c-Src to estimate p60^{src} levels (*bottom panel*). The positions of enolase and p60^{src} are indicated. *WB*, Western blot.

of Src family protein tyrosine kinases can activate these kinases (26). We tested if pORF3 had a similar effect. Control cells or cells stably expressing pORF3 were labeled with [^{32}P]orthophosphate, and the lysates were immunoprecipitated with anti-pORF3, anti-v-Src, or anti-phosphotyrosine antibodies. Two differentially phosphorylated forms of pp60^{src} (S1 and S2) were seen. While S2 was predominant in control cells (Fig. 7*A*, *lane 4*), the slower migrating S1 was predominant in pORF3-expressing cells (Fig. 7*A*, *lanes 5*, *6*, *8*, and *9*). Since S2 was missing from control (Fig. 7*A*, *lane 7*) but not from pORF3-expressing cells (Fig. 7*A*, *lanes 8* and *9*) when immunoprecipitated with anti-phosphotyrosine, we propose that this may be pp60^{src} phosphorylated at Tyr^{527}. In this inactive form of pp60^{src}, Tyr^{527} is buried in the Src SH2 domain and would therefore be inaccessible to anti-phosphotyrosine antibodies (Fig. 7*A*, *lanes 7–9*). The S1 band would then represent pp60^{src} that is dually phosphorylated at Tyr^{527} and Tyr^{416}.

Another phosphoprotein (p80) with an apparent mobility of 75–80 kDa was observed in pORF3-expressing cells but not in control cells (Fig. 7*A*, *lanes 4–9*). Since p80 was immunoprecipitated with anti-Src or anti-phosphotyrosine but not with anti-pORF3, it appeared to be associated with pp60^{src}. Anti-Src or anti-phosphotyrosine antibodies were also able to immunoprecipitate pORF3, although with poor efficiency, from ORF3–1 and ORF3–4 cells but not from control cells (Fig. 7*A*, *lanes 4–6*, *bottom panel*). This apparent inefficiency of cross-immunoprecipitation might result from only a transient intracellular association between pORF3 and pp60^{src}. Thus, there appears to be a transient trimeric complex of pp60^{src} with p80 and pORF3.

The activity of Src kinase was directly assayed by means of an immunoprecipitation kinase assay using acid-denatured enolase as a substrate. No difference was observed between control and ORF3-expressing stable cell lines (Fig. 7*B*). To ensure that the cells were capable of Src kinase modulation, they were serum-starved or activated with insulin. The Src kinase activity was found to decrease in serum-starved cells (Fig. 7*B*, *lanes 5* and *6*) and increased on insulin treatment (Fig. 7*B*, *lanes 7* and *8*) to levels observed when cells were grown in complete medium containing 10% fetal bovine serum (Fig. 7*B*, *lanes 3* and *4*). No significant change in the amount of p60^{src} protein was observed in the experiment (Fig. 7*B*, *bottom panel*).

pORF3 Expression Results in MAP Kinase Activation and Nuclear Translocation—The control and ORF3 stable cell lines were assayed for ERK activity by means of two independent assays. In a commercially available assay using the transcription factor Elk-1 as a substrate, lysates from two independent

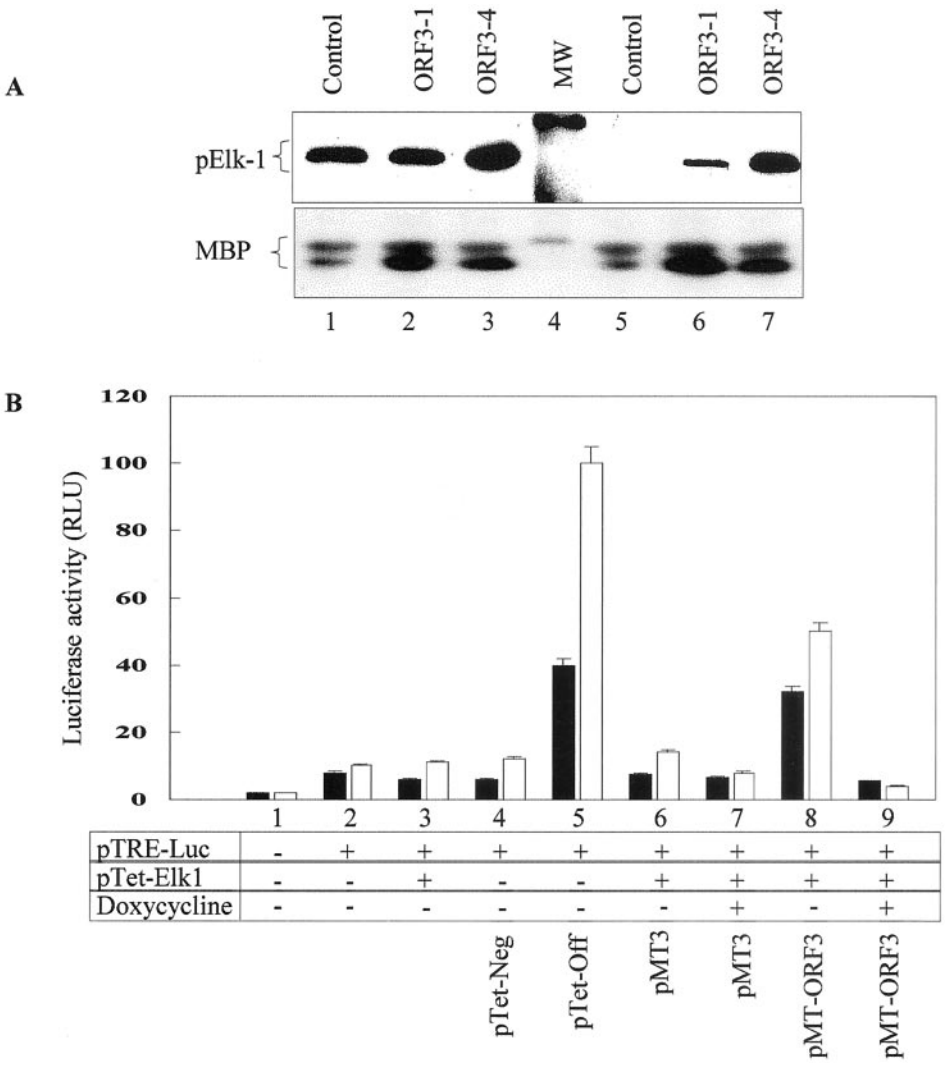

FIG. 8. **Effect of pORF3 on ERK activity.** *A*, control cells (*lanes 1* and *5*) and pORF3-expressing cells (*lanes 2*, *3*, *6*, and *7*) were grown in the presence of serum (*lanes 1–3*) or were serum-starved for 6 h (*lanes 5–7*). The lysates were then assayed for ERK activity as described under "Experimental Procedures" by means of either the p44/42 MAPK Assay System (Cell Signaling Technology) using Elk-1 as a substrate (*upper panel*) or by an immunoprecipitation kinase assay using myelin basic protein as a substrate (*lower panel*). The molecular size markers (*MW*) shown are 30 and 46 kDa (*upper panel*) and 21.5 kDa (*lower panel*). *B*, ERK activity was assayed in HEK293 (*filled bars*) and HepG2 (*open bars*) cells as described under "Experimental Procedures" by means of the *In Vivo* MAPK Assay System (CLONTECH). Cells were co-transfected with 1 μg of pTRE-Luc and 50 ng of each of the other plasmids indicated. Prior to lysate preparation, cells were serum-starved for 24 h and treated with 2 μg/ml doxycycline for 12 h where indicated. The cell lysates were assayed for luciferase activity as described under "Experimental Procedures." The results represent an average of two experiments with duplicate measurements in each experiment for all the conditions or triplicate measurements for *lanes 8* and *9*. *RLU*, relative light units.

ORF3 cell lines showed higher activity than control cells (Fig. 8*A*, *top panel*, *lanes 5–7*). However, no significant difference in the ERK activity was observed if the cells were not starved for serum prior to lysate preparation (Fig. 8*A*, *top panel*, *lanes 1–3*). In an immunoprecipitate kinase assay as well, using MBP as a substrate, increased ERK activity was observed in the ORF3 cell lines compared with the control cells (Fig. 8*A*, *bottom panel*). In this assay, however, no effect of serum starvation was observed on ERK activity.

The *in vivo* ERK activity was determined in pORF3-expressing and control cells by means of an indirect co-transfection assay. This assay relies on ERK-mediated phosphorylation of the transcription factor Elk-1 in a Tet repressor-Elk-1 fusion protein and the ability of this phosphorylated fusion protein to activate expression of a tetracycline response element (TRE)-directed luciferase reporter gene. The readout for the assay is luciferase activity in co-transfected cells. The results are shown in Fig. 7*B*. Only basal luciferase activity was observed in HEK293 or HepG2 cells co-transfected with various combinations of plasmids (Fig. 7*B*, *lanes 2–4*) except in cells co-transfected with the positive control plasmid pTet-Off and the reporter plasmid pTRE-Luc that showed about 6–10-fold induction in luciferase activity (Fig. 7*B*, *lane 5*). On co-transfection of cells with pMT-ORF3, there was about 4–5-fold induction in luciferase activity (Fig. 7*B*, *lane 8*), which was abrogated in the presence of doxycycline (Fig. 7*B*, *lane 9*). Further, co-transfection with the control expression vector pMT3 gave only basal levels of luciferase expression (Fig. 7*B*, *lanes 6* and *7*). These experiments proved conclusively that pORF3 expression can enhance ERK activity in intact cells.

The localization of MAP kinase isoforms in ORF3 cells was evaluated by indirect immunofluorescent labeling and confocal microscopy. Cells were stained with anti-p44/42 for total ERK isoforms or with anti-phospho-p44/42 for the dually phosphorylated and activated form of ERK. Cells were stained either directly after growth in serum or were first starved in serum-free medium to reduce the background of activated ERK. When stained with anti-p44/42, the control cells showed only diffuse,

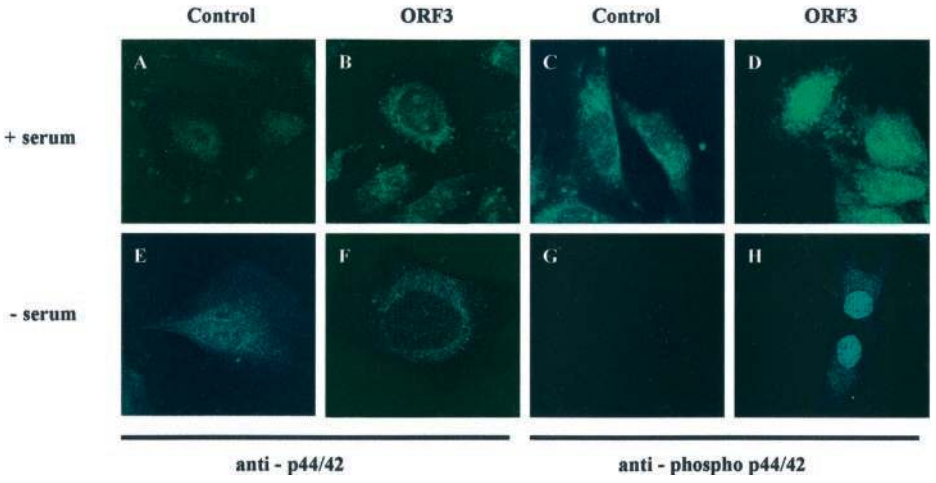

FIG. 9. **Effect of pORF3 on the localization of ERK.** Control cells (*A*, *C*, *E*, and *G*) and pORF3-expressing cells (*B*, *D*, *F*, and *H*) were grown in the presence of serum (*A–D*) or were serum-starved for 6 h (*E–H*). The cells were then fixed, stained with either anti-p44/42 (*A*, *B*, *E*, and *F*) or anti-phospho-p44/42 (*C*, *D*, *G*, and *H*) antibodies, and viewed by confocal microscopy as described under "Experimental Procedures."

nonspecific staining (Fig. 9, *A* and *E*). When stained with anti-phospho-p44/42 and when grown in serum, the control cells showed largely perinuclear staining (Fig. 9*C*); when starved for serum, these cells showed only low levels of diffuse and nonspecific staining (Fig. 9*G*). The cells expressing pORF3, on the other hand, showed cytoplasmic and largely perinuclear staining with anti-p44/42 antibodies whether grown with serum or starved of serum (Fig. 9, *B* and *F*). When the pORF3-expressing cells were stained with anti-phospho-p44/42, the signal was mainly nuclear (Fig. 9, *D* and *H*) whether the cells were grown in serum or starved of serum. These results suggest that pORF3 expression promoted translocation of the ERK subfamily of enzymes to the nucleus. Since these enzymes undergo a cytoplasm-to-nucleus translocation on activation by dual phosphorylation, which is the form of the enzyme detected with anti-phospho-p44/42 antibodies, these results further confirmed the increased activity of ERK in pORF3-expressing cells compared with control cells.

DISCUSSION

Since HEV does not grow reliably in culture, details of its biology and pathogenesis are not understood. HEV appears to be a relatively simple virus with three ORFs. Our earlier results suggested that pORF3 might be involved in modulation of the host cell (11). The types of interactions viral proteins make with cellular ones are likely to have a significant bearing on the disease process (18, 27). Here we provide the first evidence for an interaction between pORF3 and cellular proteins.

The proline-rich sequences found in the C-terminal part of pORF3 are organized into two groups of P*XX*P motifs, P-1 and P-2 (Fig. 1). Such motifs have been reported to be ligands for SH3 domains, which are conserved protein modules 50–70 amino acids long (14, 15) and are known to bind their ligands even when removed from the protein background. We tested the *in vitro* binding of pORF3 to SH3 domains from many signaling proteins that included enzymes (Src, Hck, Fyn, Csk, Abl, p85α subunit of PI3K, and PLCγ), adaptor molecules (Grb2, Crk, and p130^{cas}), and a cytoskeletal protein (Spectrin). *In vitro* binding and yeast two-hybrid assays confirmed that selected SH3 domains bound pORF3 through its P-2 region. This was further supported by dual immunofluorescent labeling, which showed colocalization of pORF3 and two SH3 domain-containing proteins, Src and Grb2.

The P-2 sequence is homologous to that of SH3 domain-binding peptide ligands and forms a type II polyproline helix with three residues per turn (14, 15). Structural and mutational studies have shown that each Xaa-Pro pair fits into a hydrophobic pocket formed by aromatic amino acids within the SH3 domain, providing the principal binding energy (28, 29). This structure is further stabilized by a salt bridge between a terminal arginine in the ligand and a conserved acidic residue in the SH3 domain (PDB 1RLQ and 1SEM). Although the exact acidic residue forming this salt bridge differs, the conservation of this interaction for the P-2 ligand indicates its importance. The SH3 ligands can bind either as class I or class II peptides depending upon whether the arginine residue is N-terminal or C-terminal to the proline-rich core (30, 31). These key structural elements were found in P-2 and provided a structural basis for its interaction with various SH3 domains. This was further confirmed by molecular modeling of the complex of c-Src or the Grb2 SH3 domain with the P-2 peptide. Based on ligand preferences of many SH3 domains (31) and the modeled structures, P-2 is likely to bind the SH3 domains as a class I peptide. Direct structural studies will address this issue in future.

Some SH3 domains bound pORF3 poorly or not at all. In Abl, the salt-bridge stabilizing aspartate is replaced by threonine (29); ligands identified by mutational analysis of Abl-SH3 domain-binding proteins 3BP1 and 3BP2 show a threonine or tyrosine instead of arginine at one end (32). The high affinity ligand for the PI3K SH3 domain is RKLPPRPSK (29). In P-2, the core is hydrophobic with a leucine instead of an arginine. This may explain the low affinity of pORF3 for the p85α SH3 domain; the PI3K ligand also binds poorly to the Src SH3 domain (29). The P-2 sequence, RPSAPPLP, is also slightly different from the high affinity SH3 binding sequence R*X*LP-P*X*P (where *X* is any amino acid) (29, 31). An extra amino acid, RPSA instead of R*X*L, N-terminal to the PP*X*P core might result in loss of binding to some but not other SH3 domains. However, sequences similar to P-2 have been identified from proteins that bind either the Src or Grb2 SH3 domains (31). Since the RPSA sequence is highly conserved between different isolates of HEV, we propose that an extra amino acid in this sequence is by design to either limit the binding efficiency of pORF3 to its cellular targets or to provide selectivity for pORF3 to bind some but not other SH3 domains.

The HIV-1 Nef is another viral protein that binds to a variety of SH3 domains (33). Nef is a high affinity ligand for the SH3 domain of Hck but not the closely related Fyn and Lck SH3 domains. While the affinity of proline-rich peptide sequences for the SH3 domains is relatively weak, with K_D values ranging from 5 to 100 μM, the Hck SH3-Nef interaction is among the strongest with a K_D value of 0.25 μM (34). The competition between pORF3 and Nef showed similar affinities of the two proteins for the Hck SH3 domain, demonstrating that pORF3 is also likely to bind SH3 ligands with an affinity in the low micromolar range.

What are the functional consequences of pORF3 binding to cellular targets? The SH3 domain-containing cellular proteins shown to bind pORF3 act upstream in the signaling pathway. Do these interactions also result in the modulation of downstream targets? For example, HIV-1 Nef binding to the SH3 domains of Src kinases results in their activation and downstream signaling leading to cellular activation (24). The hepatitis C virus NS5A protein, on the other hand, binds to the Grb2 SH3 domain and perturbs downstream mitogenic signaling (35). In ORF3 cells but not in control cells, a cellular protein (p80) was found in the $pp60^{src}$ immunoprecipitates. A similar protein, called p81, was found in the immunoprecipitates of activated but not inactive $pp60^{src}$ and has been identified as phosphatidylinositol 3-kinase (36). Although this is indicative of activated Src kinase in ORF3 cells, we were unable to detect increased activity of the Src kinase in these cells by means of a direct assay.

The activation of Src should result in the activation of downstream cellular targets and their associated physiological effects. Here we have demonstrated higher MAP kinase (ERK) activity in ORF3 cells compared with control cells by means of two independent *in vitro* assays and one co-transfection-based *in vivo* assay. Further, compared with control cells, increased levels of the dual phosphorylated form of ERK were observed in ORF3 cells. The activation of MAP kinases in cells follow Src-dependent as well as -independent pathways (37). We have also demonstrated an *in vitro* interaction between pORF3 and the SH3 domains of PI3K and PLCγ, two other enzymes that are critical modulators of downstream mitogenic signaling. In preliminary experiments, partial inhibition of ERK activity was observed in ORF3 cells treated with calphostin C, an inhibitor of protein kinase C.[2] This suggests that at least some of the pORF3 signal might transduce through the PLCγ/protein kinase C pathway.

The core (or capsid) protein of another hepatitis virus, HCV, has oncogenic potential. It has recently been shown that HCV core activates the MAPK/ERK cascade (38) and enhances activation of the transcription factor Elk-1 (39). While in one study using phospho-ERK specific antibodies there was increased phosphorylation and by analogy activity of ERK1 (38), the other study reported no ERK activation based on an immunocomplex kinase assay with the MBP as a substrate (39). Both studies used transfection-based assays, similar to the one we have used here, to establish increased activation of the ERK substrate Elk-1 (38, 39). For HCV core, therefore, it was not clear whether the Elk-1 effects were ERK-dependent or not. We have used the immunocomplex MBP assay that directly measures ERK activity and a phospho-ERK antibody-based assay that uses Elk-1 phosphorylation as a readout to show the activation of ERK in pORF3-expressing cells. We have also used the *in vivo* MAPK assay to show increased activity of Elk-1 in pORF3-expressing cells. The HCV core protein confers a growth advantage and activates a serum response element in transfected cells (40). The HEV ORF3 protein showed ERK activation in the absence or presence of serum when it was measured directly using MBP as a substrate. However, Elk-1 phosphorylation was found to be higher in pORF3-expressing cells compared with control cells only when the cells were starved of serum; in the presence of serum, no difference was observed (Fig. 8*A*). These results suggest that in the MAPK cascade, while the effects of pORF3 are largely either at or upstream of ERK, a component of the serum response might work downstream of ERK as well.

The interaction of pORF3 has been demonstrated *in vitro* with SH3 domains of proteins that are upstream modulators of three important mitogenic signaling pathways. These include the PI3K/Akt pathway, the PLCγ/protein kinase C pathway, and the Ras/Raf/MAPK/ERK kinase pathway. All these pathways lead to promotion of cell survival (41). We propose that pORF3 might function by providing an intracellular signal for cell survival. Our observation of increased activity and nuclear translocation of ERK in pORF3-expressing cells is also consistent with this hypothesis. Virus-infected cells undergo apoptosis resulting in elimination of the virus. However, an intracellular survival signal such as pORF3 would shift the balance in favor of viral replication and gene expression, thereby contributing to HEV pathogenesis. This hypothesis remains to be tested.

The presence of modular domains that mediate protein-protein interactions and contribute to signal transduction is well documented (14). Given their importance in normal cellular physiology, it is not surprising that during evolution viruses have acquired these protein modules from their eukaryotic hosts and have adapted them for their own uses. A number of viral transforming proteins utilize these modules to regulate cellular signaling resulting in uncontrolled cell growth (27). Viruses that cause latent, chronic, or persistent infections have the need to evade host immune responses. One important mechanism for achieving this is to regulate cell signaling events (18) as exemplified by the HIV or simian immunodeficiency virus Nef, the herpesvirus Samiri TIP, the Epstein-Barr virus latent membrane protein 1 and 2A (42), and the HCV core (38, 39) and NS5A proteins (35). We describe here specific interactions between the SH3 domains of several proteins involved in cell signaling and ORF3 protein of HEV, an acutely infecting virus with no reported ability to cause chronic infection or cellular transformation. To the best of our knowledge, this is the first report of such a protein-protein interaction for a virus that causes an acute and primarily self-limiting infection.

The hepatitis B virus (HBV), like HCV, is another virus linked to chronic liver disease and hepatocellular carcinoma (43). The HBx protein of hepatitis B virus has also been shown to activate the MAPK pathway, primarily by activating formation of a Ras·GTP complex (44). The observations on HBx (44) and HCV core (38, 39) together with our results on the HEV ORF3 protein presented in this report suggest activation of the MAPK cascade as a common theme for hepatitis viruses. This would offer a growth advantage to virus-infected cells. Why hepatitis B virus and HCV progress to chronic hepatitis and hepatocyte transformation while HEV causes an acute and self-limiting infection is an interesting question to which we have no answers at this time.

Acknowledgments—We are grateful to Ivan Gout, Michael Waterfield, Ruibao Ren, and Jonathan Chernoff for contributing the GST-SH3 fusion constructs; Albert Tam and Genelabs Technologies for the Mexican isolate ORF3 plasmid; and Amit Sharma for suggestions on the homology modeling.

REFERENCES

1. Purcell, R. H. & Ticehurst, J. R. (1988) in *Viral Hepatitis and Liver Disease* (Zuckerman, A. J., ed) pp. 131–137, Alan R. Liss, New York
2. Ramalingaswami, V. & Purcell, R. H. (1988) *Lancet* **1,** 571–573
3. Krawczynski, K. (1993) *Hepatology* **17,** 932–941
4. Panda, S. K. & Jameel, S. (1997) *Viral Hepat. Rev.* **3,** 227–251
5. Nanda, S. K., Yalcinkaya, K., Panigrahi, A. K., Acharya, S. K., Jameel, S. & Panda, S. K. (1994) *J. Med. Virol.* **42,** 133–137
6. Lau, J. Y. N., Sallie, R., Fang, J. W. S., Yarbough, P. O., Reyes, G. R., Portmann, B. C., Mieli-Vergani, G. & Williams, R. (1995) *J. Hepatol.* **22,** 605–610
7. Khuroo, M. S., Teli, M. R., Skidmore, S., Sofi, M. A. & Khuroo, M. (1981) *Am. J. Med.* **70,** 252–255
8. Nayak, N. C., Panda, S. K., Datta, R., Zuckerman, A. J., Guha, D. K., Madangopalan, N. & Buckshee, K. (1989) *J. Gastroenterol. Hepatol.* **4,** 345–352
9. Panda, S. K., Nanda, S. K., Zafrullah, M., Ansari, I. H., Ozdener, M. H. & Jameel, S. (1995) *J. Clin. Microbiol.* **33,** 2653–2659
10. Jameel, S., Zafrullah, M., Ozdener, M. H. & Panda, S. K. (1996) *J. Virol.* **70,** 207–216

11. Zafrullah, M., Ozdener, M. H., Panda, S. K. & Jameel, S. (1997) *J. Virol.* **71,** 9045–9053
12. Zafrullah, M., Ozdener, M. H., Kumar, R., Panda, S. K. & Jameel, S. (1999) *J. Virol.* **73,** 4074–4082
13. Tam, A. W., Smith, M. M., Guerra, M. E., Huang, C. C., Bradley, D. W., Fry, K. E. & Reyes, G. R. (1991) *Virology* **185,** 120–131
14. Pawson, T. (1995) *Nature* **373,** 573–580
15. Cohen, G. B., Ren, R. & Baltimore, D. (1995) *Cell* **80,** 237–248
16. Koch, C. A., Anderson, D., Moran, M. F., Ellis, C. & Pawson, T. (1991) *Science* **252,** 668–674
17. Mayer, B. J. (1999) in *Signaling Networks and Cell Cycle Control* (Gutkind, J. S., ed) pp 439–452, Humana Press, Totowa, NJ
18. Krajcsi, P. & Wold, W. S. M. (1998) *J. Gen. Virol.* **79,** 1323–1335
19. Ahmad, K. M., Mujtaba, S., Das, R., Zafrullah, M., Sehgal, S. & Jameel, S. (1998) *AIDS Res. Hum. Retrovir.* **14,** 1491–1493
20. Rosenberg, I. M. (1996) in *Protein Analysis and Purification*, pp. 343–344, Birkhauser, Boston
21. Fields, S. & Song, O. (1989) *Nature* **30,** 245–246
22. Rose, M. D., Winston, F. & Hieter, P. (1990) *Methods in Yeast Genetics*, Cold Spring Harbor Laboratory, Cold Spring Harbor, NY
23. Cornell, W. D., Cieplak, P., Bayly, C. I., Gould, I. R., Merz, K. M., Ferguson, D. M., Spellmeyer, D. C., Fox, T., Caldwell, J. W. & Kollman, P. A. (1995) *J. Am. Chem. Soc.* **117,** 5179–5197
24. Sicheri, F., Moarefi, I. & Kuriyan, J. (1997) *Nature* **385,** 602–609
25. Wittekind, M., Mapelli, C., Farmer, B. T., Suen, K.-L., Goldfarb, U., Tsao, J., Lavoie, T., Barbacid, M., Myers, C. A. & Mueller, L. (1994) *Biochemistry* **33,** 13531–13539
26. Moarefi, I., LaFevre-Bernt, M., Sicheri, F., Huse, M., Lee, C.-H., Kuriyan, J. & Miller, W. T. (1997) *Nature* **385,** 650–653
27. Bliska, J. (1996) *Chem. Biol.* **3,** 7–11
28. Feng, S., Chen, J. K., Yu, H., Simon, J. A. & Schreiber, S. L. (1994) *Science* **266,** 1241–1246
29. Yu, H., Chen, J. K., Feng, S., Dalgarno, D. C., Brauer, A. W. & Screiber, S. L. (1994) *Cell* **76,** 933–945
30. Lim, W. A., Richards, F. M. & Fox, R. O. (1994) *Nature* **372,** 375–379
31. Sparks, A. B., Rider, J. E., Hoffman, N. G., Fowlkes, D. M., Quilliam, L. A. & Kay, B. K. (1996) *Proc. Natl. Acad. Sci. U. S. A.* **93,** 1540–1544
32. Ren, R., Mayer, B. J., Cicchetti, P. & Baltimore, D. (1993) *Science* **259,** 1157–1161
33. Saksela, K., Cheng, G. & Baltimore, D. (1995) *EMBO J.* **14,** 484–491
34. Lee, C.-H., Leung, B., Lemmon, M. A., Zheng, J., Cowburn, D., Kuriyan, J. & Saksela, K. (1995) *EMBO J.* **14,** 5006–5015
35. Tan, S.-L., Nakano, H., He, Y., Vijaysri, S., Neddermann, P., Jacobs, B. L., Mayer, B. J. & Katz, M. G. (1999) *Proc. Natl. Acad. Sci. U. S. A.* **96,** 5533–5538
36. Courtneidge, S. A. & Heber, A. (1987) *Cell* **50,** 1031–1037
37. Burgering, B. M., de Vries-Smits, A. M., Medema, R. H., van Weeren, P. C., Tertoolen, L. G. & Bos, J. L. (1993) *Mol. Cell. Biol.* **13,** 7248–7256
38. Hayashi, J., Aoki, H., Kajino, K., Moriyama, M., Arakawa, Y. & Hino, O. (2000) *Hepatology* **32,** 958–961
39. Fukuda, K., Tsuchihara, K., Hijikata, M., Nishiguchi, M., Kuroki, T. & Shimotohno, K. (2001) *Hepatology* **33,** 159–165
40. Tsuchihara, K., Hijikata, M., Fukuda, K., Kuroki, T., Yamamoto, N. & Shimotohno, K. (1999) *Virology* **258,** 100–107
41. Shimamura, A., Ballif, B. A., Richards, S. A. & Blenis, J. (2000) *Curr. Biol.* **10,** 127–135
42. Collette, Y. & Olive, D. (1997) *Immunol. Today* **18,** 393–400
43. Schafer, D. F. & Sorrell, M. F. (1999) *Lancet* **353,** 1253–1257
44. Benn, J. & Schneider, R. J. (1994) *Proc. Natl. Acad. Sci. U. S. A.* **91,** 10350–10354